THE STUDY OF WING-ROCK CHARACTERISTICS ON SLENDER DELTA WINGS AT HIGH AOA

Fei-Bin Hsiao and Jiue-Sheng Yang

Institute of Aeronautics and Astronautics, National Cheng Kung University

Tainan, Taiwan, China

Abstract - The oscillatory rocking characteristics of delta-shaped, slender wings at high angles of attack (AOA) are experimentally studied in a low subsonic wind tunnel. The wing models investigated include single-delta and double-delta planforms. A rotary variable differential transformer is used as a sensing element to respectively measure the rolling angle variations of the models. The free-to-roll tests are first conducted at various AOA and freestream velocity. Results indicate that the model, as being increased to some high AOA, behaves as a self-induced oscillatory roll motion which is independent of the initial disturbance angle imposed, while the rate of contraction of the roll motion is clearly influenced by the imposed initial rolling angle, rolling moment of inertia, and freestream velocity. From the results of the rocking frequency and amplitude of the oscillations, two features of the reduced frequency are obtained for SD wings: a constant region with a bell-shaped form for the 80° delta wings, and a linear-varying region for the 75° delta wing. However, a well-collapsed curve of both features are obtained for the DD wing.

Introduction

In modern air combat tactics, the jet fighter's agility, maneuverability and survivability are vitally important to differentiate the triumph from defeat in the battle. During the close-contact air fighting, the aircraft must have ability to perform such as sharp turning and rapid climb at some speeds for attacking or escaping. Accordingly, the aircraft has to increase its flying angle of attack (AOA) so as to produce enough lift and drag forces. It is thus a necessity of the aircraft that such high lift force shall be ensured to maintain its high performance and refrain from wing stall at this high AOA flight. For the delta-wing aircraft, it fortunately bears the characteristics that the lift force can be maintained at the AOA much higher than the conventional straight-wing aircraft, and that the stall angle can reach as high as 35° before the wing stall takes place and the lift starts to drop off after the post-stall angle. In fact, this is one of the reasons why the delta-wing aircraft owns the better aerodynamic performance than that of the straight-wing aircraft as flying at high speed, and is thus favorably used in the jet fighters[1]. Besides beneficial from the use of the highly swept delta-shaped wing for the jet fighters, yet there exists some limitations and constraints associated with the flying qualities, which may deteriorate the flight performance and thus limits the applicability of the delta-shaped aircraft. Among those drawbacks, the lateral self-induced unstable oscillations in roll motion may take place especially when the aircraft flies at high angles of attack. This so-called wing rock phenomenon is a limit-cycle oscillation occurred in the lateral direction and may easily be coupled with the laterally yawing motion. As soon as this unstable motion occurs, the aircraft's lift will reduce all of a sudden[2], resulting in loosing flying performance and lost control of maneuver. It thus shows an important issue of study on wing rock motion for a delta-shaped wing at high angles of attack.

Since the wing-rocking motion of a delta-shaped wing mainly comes from the highly nonlinear aerodynamic properties, the flow field in association with the wing planform to causing this oscillatory motion plays the major role in terms of mechanism and process to initiate this motion. However, although the external flow field may be dependent upon the configuration of the wing, this rocking motion is virtually originated from the unsymmetric vortical structures on the upper surface of the wing to create unbalanced lifts on both sides of the wing; the rocking motion in roll is thus created. Following the study of Ericsson and Reding[3] for a slender delta wing at high angle of attack, many researchers placed emphasis on the simulation and experimental studies for this high-amplitude unstable rolling motion at high AOA. Levin and Katz[2] employed a 80° swept-backward delta wing to study the wing rock phenomenon through the wing tunnel testing, concluding that the rocking frequency and amplitude of the oscillatory motion bear strong relationship with the angle of attack and the freestream velocity. This rocking motion was also studied by Schmidt[4] and Nguyen, et al.[5], and

three possible mechanisms to result in wing rocking were proposed, which includes the loss of roll damping, static nonlinear aerodynamics, and aerodynamic hysteresis. This conjecture was further modified by Ericsson[6,7] as stressing that the generation of vortex asymmetry on the upper surface of the wing was the major mechanism for producing such roll motion in stead of the vortex bursting. He further emphasized that the vortex asymmetry was prior to occur than the vortex bursting for a slender delta wing in terms of the angle of attack. This roll motion is thus conceived as a self-induced oscillations due to flow separation from the leading edges of the delta wing to form two unsymmetric, spiral vortices with respect to the roll axis of the wing. These two vortical structures are intimately linked with the incipience of the aerodynamic hysteresis, which was proclaimed to provide the roll moment for persistent, roll-oscillatory motion[5]. While the vortices are bursting into small eddies as the angle of attack gets very high, the storing moment for roll motion will disappear and thus the roll motion will be diminished. Ericsson[7] thus concluded that vortex bursting is a dynamically stabilizing effect to inhibit the amplitude growth of the roll motion.

In modern jet fighters, the delta wing is usually embedded with a cylinder body to form a wing-body combination. This forebody design of the fighter is necessary for carrying avionics and armaments. Ericsson[8,9] thought that the cylindrical forebody ahead of the delta wing would naturally create small-scaled turbulence to enhance vortex asymmetry, thus the wing rock unstable motion was further manifested. Hence, the geometrical consideration of the forebody in terms of the wing rock motion falls a very important factor in fighter design.

From the literature survey as discussed above, it is understood that the flow field vortical structures are closely correlated with the mechanism for creating the unstable roll motion for a delta wing at high AOA. However, it still remains unclear about the frequency and amplitude of the roll motion in association with the angle of attack, freestream velocity, and rolling moment of inertia of the delta wing, in which these parameters usually play the important roles in investigating the wing rock characteristics. Apart from the slender single-delta wings will be studied, slender double-delta wings in simulation of the forebody effect on the delta wing will also be used to further investigate the deterministic properties of the wing rocking motion.

Experimental Apparatus and Procedures

The experiments are conducted in a subsonic, open-type wind tunnel with a test section of 90 x 120-cm. The maximum air speed in the test section is 30 m/sec with the turbulence level less than 1%. Two kinds of test models are used throughout the investigations, the single delta (SD) and double delta (DD) slender wings. As illustrated in Fig. 1, both delta wings are designed and manufactured to have the swept-backward angle of 75° and 80° (equal to semi-apex angle 15° and 10°, respectively) for SD wings, and the combination of both for DD wings. Both SD and DD models are beveled 45° sharply downward at the leading edges so as to easily create the leading-edged, separation vortices which then shed downstream on the upper surface of the wing. All models tested are 2 mm in thickness and 330 mm in maximum chord length, while the wing span (B) varies accordingly due to different swept angles used. It is noted that not only both Aluminum alloy and Carbon Steel are used for the models, but also some central parts of the models are replaced by dead weights in a symmetric way. This is convenient to vary the moment of inertia in longitudinal axis (called I_{xx}) for tests. The detailed dimensions, main material used, and the corresponding abbreviated tag-names of the models are listed in Table 1 for comparison.

A free-to-roll mechanism, as shown in Fig. 2, is designed to support the wing model in a limited oscillation range of $\pm 90^0$. The mechanism is also able to control the center of mass of the model always located in the central portion of the test section when the angle of attack varies, so that the wind tunnel wall effect is supposedly diminished to some degree. In the current experiments, the angle of attack ranges between 20° and 60°. The rolling angle signals in time are obtained by connecting a fast-response angle sensor, called rotary variable differential transformer (RVDT), to the end of the model's rolling arm, which is then fed into a PC-486 computer through an A/D converter with the maximum sampling rate 50 KHz. The linear range of the RVDT angle response is between ± 65°. In the meantime, a FFT spectrum analyzer is also employed to calculate and plot the frequency response directly from the RVDT outputs.

Experimental Results and Discussion

On-set Behavior of the Wing Rock Oscillations

As discussed in the previous section, the unsymmetric vortices over the upper surface of the wing at high AOA are generated due to externally imposed disturbance roll angle, which may induce the on-set oscillations of the wing rocking motion. The wing may just oscillate for a few cycles and then diminish its amplitude to zero in the long run as shown in Fig. 3-a for the model SD80-4 operated at 24° AOA. In this case, the

wing rocking motion is in dynamic stability where the initial rolling moment from the imposed disturbance angle is damped out by the system. Fig. 3-a also clearly shows the stable oscillations that the model reduces its amplitude to zero after it is imposed by a 10° roll angle. However, when the AOA increases to 25° and more large disturbance angle is imposed as shown in Fig. 3-b, the wing rocking motion is then persistent and gets saturated in amplitude after many cycles. This is commonly called the limit-cycle oscillations. The temporal evolution of the amplitude variations can be given by a formula composed of the logarithmic envelop and the sinusoidal oscillation, as follows:

$$A = A_0(1 - e^{-\lambda t})\sin(2\pi F t) \qquad (1)$$

where A denotes the amplitude at any instant of time t, A_0 the saturated amplitude, λ the rate of contraction, and F the rocking frequency of the model. The rate of contraction is positive when the amplitude of oscillations increases with time, and thus λ stands for the convergence rate of the wing rocking system to saturation. The larger the λ is, the less the damping of the system will be, so that the less stable the system will be and hence easier to be disturbed. Through the parametric analysis of the wing rocking system, the rate of contraction behaves as a function of initial disturbance angle ($\Delta\Phi$), moment of inertia (I_{xx}), and freestream velocity (V). Fig. 4 shows the effect of $\Delta\Phi$ on the value of λ for SD80-4 model. It is surprising to note that although $\Delta\Phi$ only varies from 7° to 10°, the corresponding values of λ change from 0.28511 to 0.62781. Fig. 4 also shows that the saturated amplitude keeps the same although the initial disturbance angles are different. The same results are also shown in the subsequent figures in terms of the angle of attack. Thus, we can conclude one thing here that the extreme saturated amplitude of the wing rock limit cycle oscillation is independent of the initial imposed disturbance angle. Fig. 5 shows the effect of moment of inertia on the rate of contraction, indicating that the larger the I_{xx} is, the less the λ will be, and hence more stable the system is. Thus, for a wing with large moment of inertia, the wing rock will take longer time to reach the saturated, limit cycle of oscillations. Meanwhile, as the freestream velocity increases, the rate of contraction will also increase, but with less significant as compared to the other two parameters above. From Figs. 4 and 5 for the model SD-80 tests and the SD-75 tests but not shown here, we can conclude that the rate of contraction is strongly influenced by the initial disturbance angle, while the influence by the moment of inertia is the less, and by the freestream velocity the least.

Wing Rock Oscillations as a Function of AOA

The nature of limit cycle oscillations of wing rock is clearly manifested as discussed in the previous section. However, it still remains unclear how the frequency and amplitude of the wing rock varies in terms of the angle of attack. We thus conduct the wing rock experiments of all models by varying the angle of attack from 24° to 60°. The typical rolling oscillations for SD80-4 model are depicted in Fig. 7 at various AOA. It clearly shows that before AOA equals 34°, the wing oscillates in a constant amplitude feature. After AOA is greater that 34°, some amplitude modulations are pronounced and the amplitude of oscillations reduces with AOA. Until AOA reaches 50° or higher, the wing rock almost ceases oscillation especially when AOA exceeding 58° or so. This is a phenomenon of the so-called vortex breakdown to cause the wing model becoming more stable or just a light vibration as was discussed by Ericsson[9]. This phenomenon is also obtained in the investigations of both SD80 and SD75 models. Fig. 8 presents the data of SD80-1 model using rocking frequency and amplitude as parameters but tested in various freestream velocities. Results indicate that the rocking frequency increases with the increase of the freestream velocity, while the rocking amplitude almost keeps constant with the variations of the freestream velocity tested. It is also noted that the rocking frequency almost keeps constant with AOA to some degrees and then steeply increases and decreases afterwards. The rocking frequency is hardly detected when the amplitude of oscillations approaches zero, as was discussed in Fig. 7. Thus, we can differentiate two regions of frequency variations in the wing rock behavior, which was also noted by Levin and Katz[2] and Nguyen, et al.[5] in their experiments. The first region corresponds to the constant frequency region where the rocking amplitude keeps increasing until reaching the maximum. In this linear region, Ericsson[6] explained that the leading-edged vortices on the upper surface behave the interchanging process of either vortex lift-off or reattachment to the wing surface. The vortex breakdown location will move upstream from the trailing edge of the wing with the increase of the AOA until the breakdown location reaches the apex of the delta wing where the wing stall or massive separation subsequently occurs. After exceeding the maximum amplitude, the rocking frequency starts to increase sharply while the amplitude starts to decrease accordingly, and the flow on the upper surface of the wing behaves in a fashion of massive flow separation that the rocking frequency ceases oscillating and zero amplitude was measured. Thus, the variable-frequency region is corresponding to such case that the flow starts to separate from the wing surface initially from the trailing edge where the constant-frequency region ends and the variable-frequency regions sets off, to the leading edge where the variable-frequency region terminates. This feature was also obtained in all SD80 models tested. While for SD75-1 model as shown in Fig. 9, the apex angle is

increased to 15° where a large amount of vorticity of the separation vortices is accumulated near the apex so that the unsymmetric vortex breakdown is easy to occur, as was visualized by Morris and Ward[10] at the same apex angle and flow conditions. This will cause the rocking frequency varies in the fashion different from the SD80 series, and the frequency appears to vary linearly with the AOA until the oscillations diminish at some AOA where the rocking amplitude reduces its value sharply as well.

As for the wing rock behavior of the double-delta (DD) wing model, it was discussed previously that the first part (forward) of the delta wing will behave like the strake of a forebody to induce the strake vortices which will shed downstream to undergo interactions with the latter separation vortices created on the second part of the delta wing. In some cases, the former strake vortices may be stronger in strength than the latter wing vortices, so that the former may govern the entire flow characteristics. However, both vortices will merge together before reaching the end of the wing model. This kind of flow characteristics will be determined by the apex angle and AOA, as presented by Erisson[9]. Fig. 10 collects the wing rock oscillations for model DD from 21° to 60° of AOA. At 21°, the wing motion is dynamically stable. While beyond that angle, the wing rock starts to occur and the corresponding amplitude keeps increasing and decreasing depending upon the AOA. The values of the associated frequency and amplitude are calculated and plotted in Fig. 11 in terms of various freestream velocities. It is noted that the DD model is composed of the 80° swept-backward at the first half and 75° at the second half of the model. As aforementioned discussion, the vortices generated in the strake may govern the entire flow field characteristics of the vortex development. Hence, the results of frequency and amplitude variations with AOA for the DD model behave a feature close to those for the SD80 model. It is also noted that although the existence of the strake will increase the wing lift[11], the strake will also reduce the initial AOA for wing rock oscillations. That is, the strake is a destabilizing device to cause the wing apt to rock. This is clearly a drawback when the strake is installed to the forebody of an aircraft in comparison to the benefit of the wing strake for the high-lift augmentation.

Non-dimensional Characteristics of Wing Rock Oscillations

Hsu and Lan[12] studied the wing rock behavior using a simplified theoretical approach to obtain the rocking frequency in terms of relevant flow parameters. However, as the AOA increases to some value where the vortex bursting occurs on the upper surface of the wing, the flow behaves nonlinearly and this theory can no longer predict the rocking frequency accurately. However, through Hsu and Lan[12] analysis, we could conceive the important parameters which may be involved with the wing rock oscillations. Among them, the relevant parameters will include as given in Eq. (2)

$$F = f\ (V, AOA, I_{xx}, B, \theta_A, \Delta\theta, m) \qquad (2)$$

After non-dimensional analysis, Eq. (1) can be reformed to give Eq. (3)

$$Fr = \frac{FB}{V} = f\ (\frac{I_{xx}}{mB^2}, AOA, \Delta\theta, Re, \Delta\theta) \qquad (3)$$

where Fr is called the reduced frequency, I_{xx}/mB^2 the reduced moment of inertia, m the mass of the model, Re the Reynolds number based on wing span B. In this paper, the parameters of the apex angle θ_A and the initial disturbance angle $\Delta\theta$ are kept constant without detailed investigations. Due to the speed limit of the wind tunnel facility, the freestream velocity tested ranges from 15 to 25 m/s, which is almost at the same order of magnitude. Nevertheless, the rest of the parameters are carefully studied and presented for comparison. Fig. 12 shows the variations of the reduced frequency with AOA for four SD80 models. In each figure, the experimental data in terms of AOA are well collapsed in terms of the wind velocity operated. The constant-frequency region and the variable-frequency regions are also well defined as discussed before. As for the SD75 models shown in Fig. 13, the data showing the reduced frequency with AOA also collapse pretty well for all wind speed. The reduced frequency with AOA for the DD model also presents the same feature of all data collapse into one curve as depicted in Fig. 14. In comparison of the experimental reduced frequency between SD and DD models, Fig. 15 shows the variations of the averaged value of the reduced frequency (Frav) with AOA. Note that only the constant-frequency region is illustrated for detailed comparison. It can be seen that the reduced frequencies for the SD75 models are higher than those for the SD80 models. As the moment of inertia is increased, the reduced frequency is decreased accordingly for both SD75 and SD80 models. As for the DD model, its reduced frequency features similarly to the SD80 models but has the higher value than the SD80 model at the same moment of inertia. If only the constant-frequency range is compared, Fig. 16 will show that the reduced frequency is almost in linear reciprocal with the reduced moment of inertia. That is, the product of the reduced frequency and the reduced moment of inertia will keep almost constant in the investigations.

Concluding Remarks

In this study, the free-to-roll tests have been carried out for the investigations of the wing rock

characteristics on the flat-plate delta wings in a subsonic wing tunnel. Both single delta (SD) and double delta (DD) wing models are exploited with regard to the on-set oscillations of the wing rock, the frequency and amplitude properties of oscillations, and their non-dimensional properties of the reduced frequency and amplitude in relation to the parameters studied. Results indicated that the wing rock phenomenon is a self-induced oscillatory rolling motion, which is independent of the initial disturbance roll angle. The experimental results of the rate of contraction shows a good measure of instability for a delta wing undergoing self-induced roll oscillations, which is influenced by external roll disturbance angle, moment of inertia, and the wind speed. The reduced frequencies for both SD and DD models are well collapsed, respectively, under non-dimensionalization. The product of the reduced frequency and the reduced moment of inertia gives almost a constant value. From the test of DD model, it shows that the use of strake has strong influence on the wing rock characteristics and the initial AOA for wing rock oscillations will be reduced as well.

Acknowledgment

This work is supported by the National Science Council R.O.C. under Contract no. NSC 82-0410-D-006-017.

References

1. Polhamus, E. C., "Applying Slender Wing benefits to Military Aircraft," Journal of Aircraft, Vol. 21, No. 8, Aug. 1984, pp. 545-559.

2. Levin, D. and Katz, J., "Dynamic Load Measurements with Delta Wings Undergoing Self-induced Roll Oscillations," J. of Aircraft, Vol. 21, No. 1, Jan. 1984, pp. 30-36.

3. Ericsson, L. E. and Reding, J. P., "Unsteady Aerodynamics of Slender Delta Wings at Large Angle of Attack," J. of Aircraft, Vol. 12, No. 9, Sep. 1975, pp. 721-729.

4. Schmidt, L. V., "Wing Rock Due to Aerodynamic Hysteresis," J. of Aircraft, Vol. 16, No. 3, March 1979, pp. 129-133.

5. Nguyen, L. T., Yip, L. P. and Chambers, J. R., "Self-induced Wing Rock of Slender Delta Wings," AIAA Paper no. 81-1883, Aug. 1981.

6. Ericsson, L. E., "The Fluid Mechanics of Slender Wing Rock," J. of Aircraft, Vol. 21, No. 5, May 1984, pp. 322-328.

7. Ericsson, L. E., "Sources of High Alpha Vortex Asymmetry at Zero Sideslip," J. of Aircraft, Vol. 29, No. 6, Nov.-Dec. 1992.

8. Ericsson, L. E. and Reding, J. P., "Dynamics of Forebody Flow Separation and Associated Vortices," J. of Aircraft, Vol. 22, No. 4, April 1985, pp. 329-335.

9. Ericsson, L. E., "Various Sources of Wing Rock," J. of Aircraft, Vol. 27, No. 6, June 1990, pp. 488-494.

10. Morris, S. L. and Ward, D. T., "A Video-Based Experimental Investigation of Wing Rock," AIAA 89-3349-CP.

11. Ho, C. M. and Lee, M., "Lift Force of Delta Wings," Applied Mech. Review, Vol. 43, No. 9, Sep. 1990, pp. 209-221.

12. Hsu, C. H. and Lan, C. E., "Theory of Wing Rock," AIAA Paper no. 85-0199, Jan. 1985.

Table 1: Specifications of testing models

	θ_A	C (mm)	B (mm)	t (mm)	Material	m (g)	I_{xx} (g-cm^2)	S (cm^2)
SD80-1	10°	330	116	2	Al	100	557.3	191.4
SD80-2	10°	330	116	2	Al	110	646.8	191.4
SD80-3	10°	330	116	2	Al	144	984.8	191.4
SD80-4	10°	330	116	2	Steel	310	1,912	191.4
SD75-1	10°	330	172	2	Al	110	1,527	283.8
SD75-2	10°	330	172	2	Al	125	1,663	283.8
SD75-3	10°	330	172	2	Al	160	2,123.3	283.8
Double Delta	$\theta_s = 10°$	330	$B_s = 81$	2	Al	115	818	200.65
	$\theta_w = 15°$		$B_w = 134$					

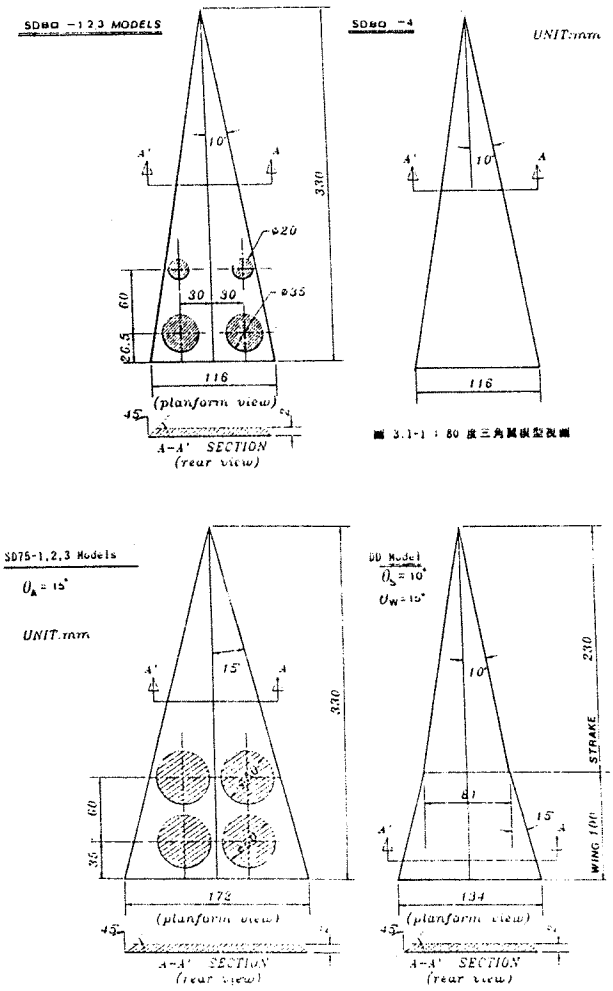

FIGURE 1 - Dimensions of the delta wing models

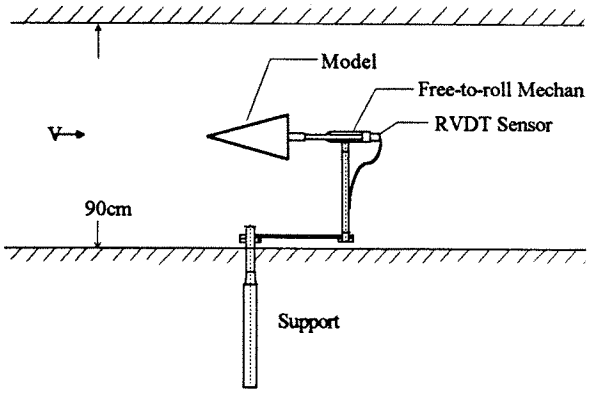

FIGURE 2 - Wing tunnel test arrangement

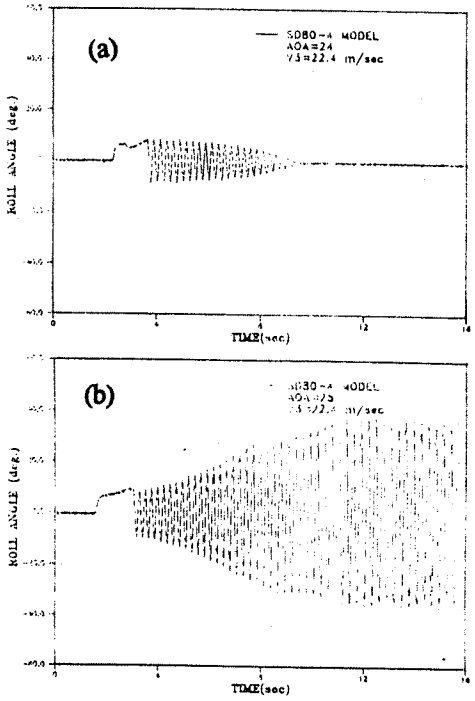

FIGURE 3 - On-set behavior of SD80-4 model for 22.4 m/s and (a) 24°, (b) 25° AOA

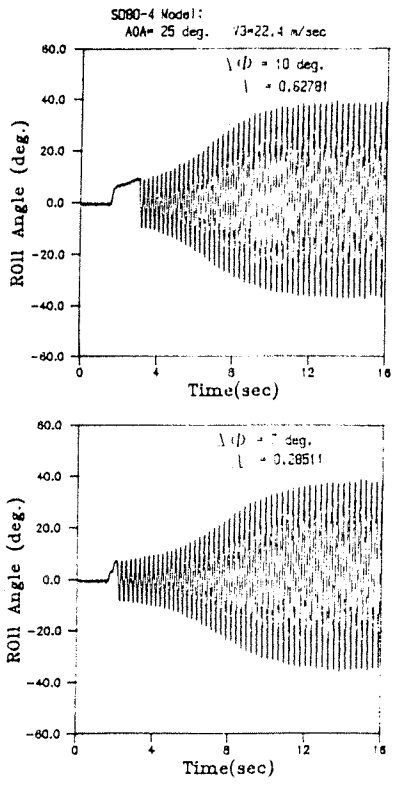

FIGURE 4 - Effect of initial disturbance angle on rate of contraction at 25° AOA and 22.4 m/s for SD80-4 model

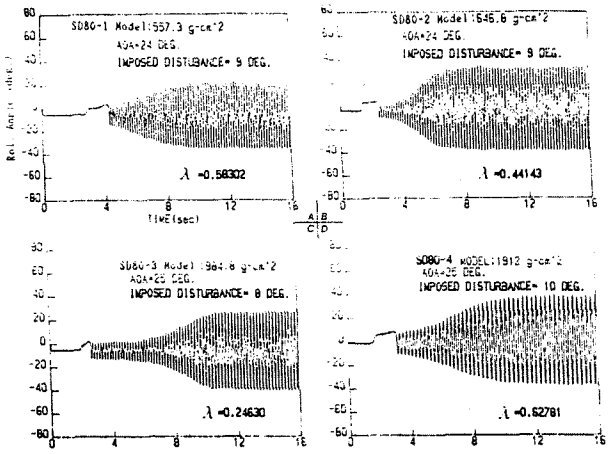

FIGURE 5 - Effect of rolling moment of inertia on rate of contraction at 22.4 m/s for SD80 models

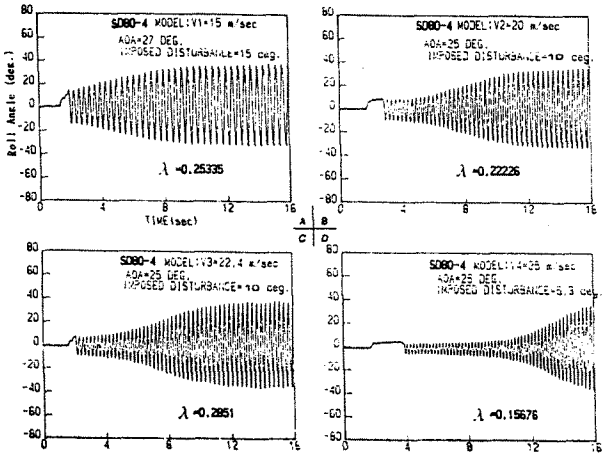

FIGURE 6 - Effect of wing speed on rate of contraction for SD80-4 model

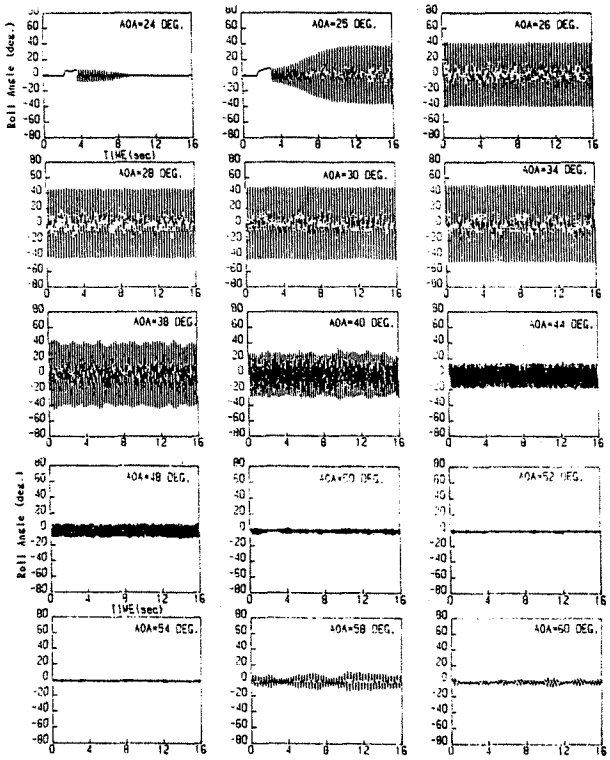

FIGURE 7 - Wing rock oscillations in terms of AOA at 22.4 m/s for SD80-4 model

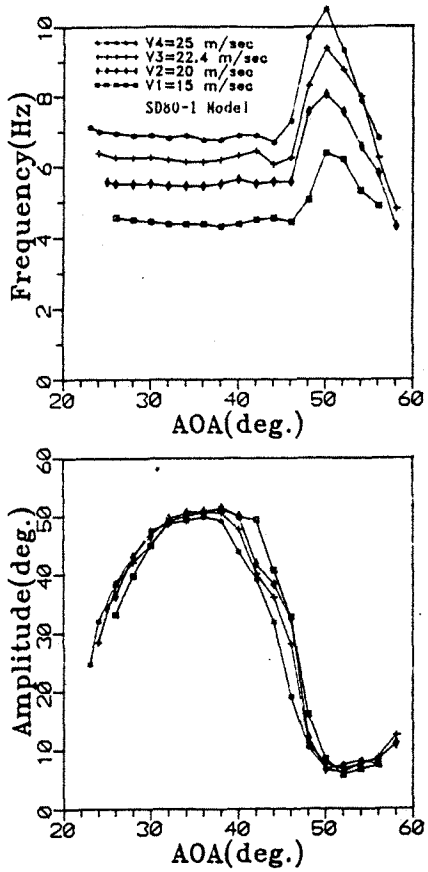

FIGURE 8 - Rolling frequency and amplitude with AOA at various wind speeds for SD80-1 model

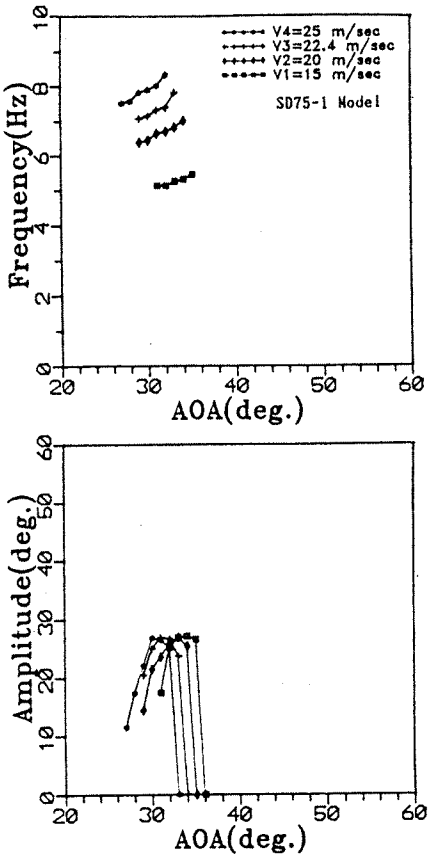

FIGURE 9 - Rolling frequency and amplitude with AOA at various wind speeds for SD75-1 model

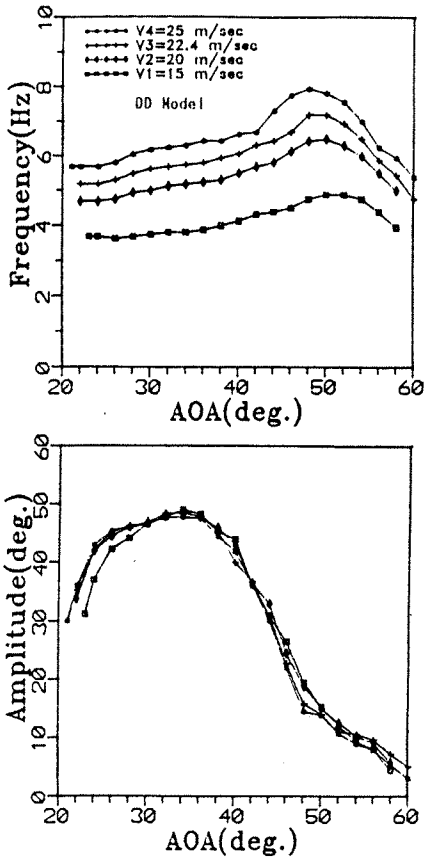

FIGURE 11 - Rolling frequency and amplitude with AOA at various wind speeds for DD model

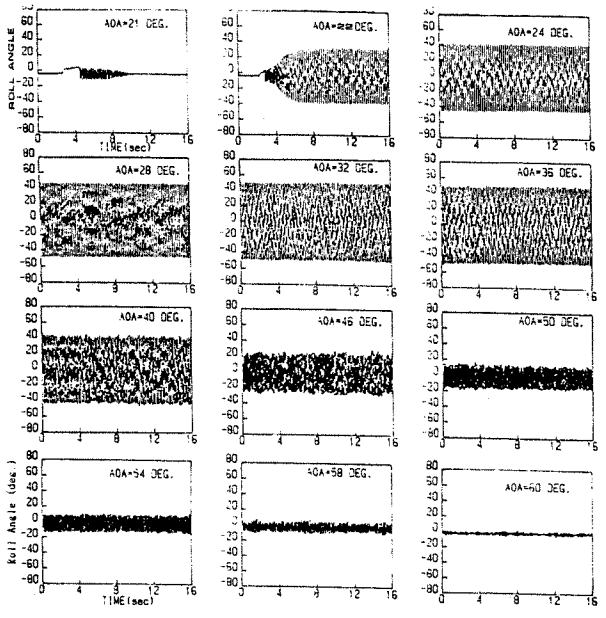

FIGURE 10 - Wing rock oscillations in terms of AOA at 22.4 m/s for DD model

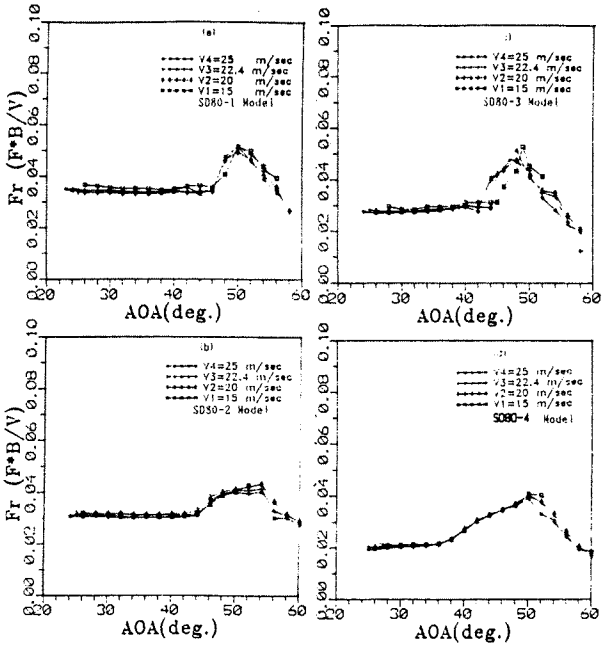

FIGURE 12 - Reduced rocking frequency with AOA at various wind speed for SD80-2 model

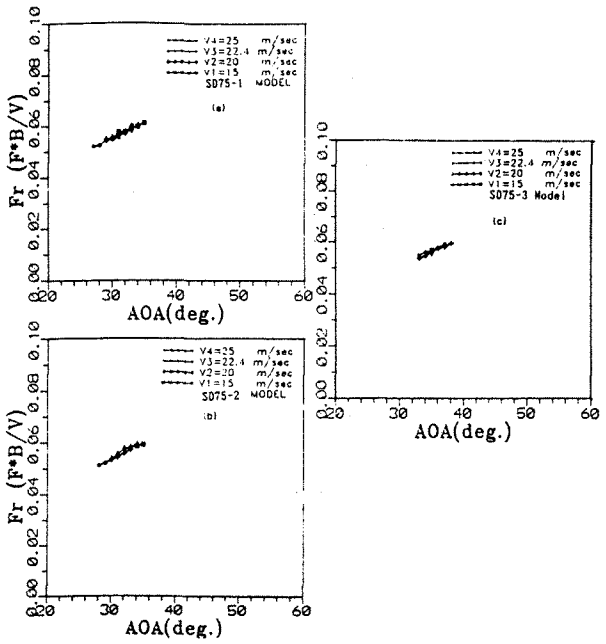

FIGURE 13 - Reduced rocking frequency with AOA at various wind speed for SD75-2 model

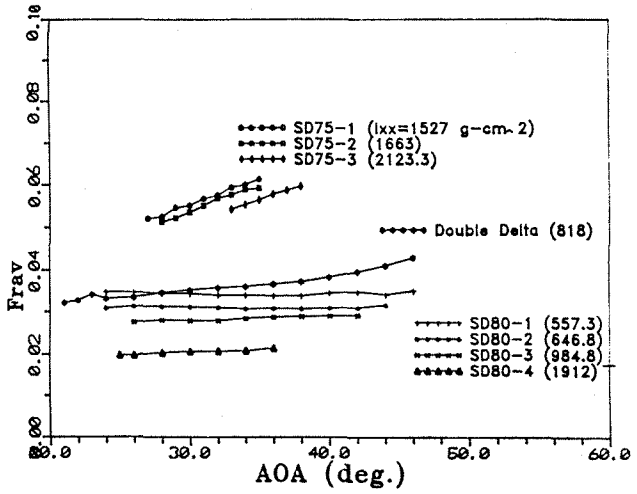

FIGURE 15 - Comparisons of averaged reduced frequency with AOA for SD and DD models

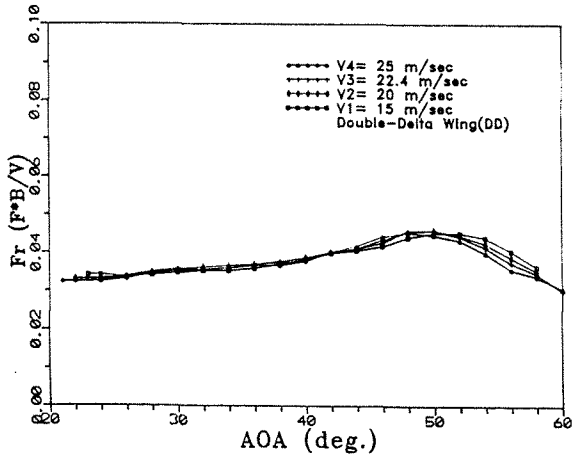

FIGURE 14 - Reduced rocking frequency with AOA at various wind speed for DD model

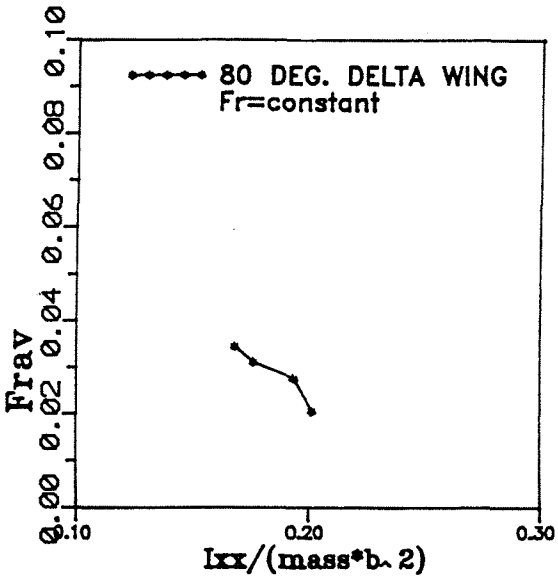

FIGURE 16 - Averaged reduced frequency with reduced rolling moment of inertia for SD80 models